Aerodynamic analysis of Blade NACA 65_3-218 of Horizontal Axis Wind Turbine (HAWT) using Computational Fluid Dynamics

Abdur Rahim[1] and Satyam Dewivedi[2]

[1]Faculty, Department of Mechanical Engineering Jamia Milia Islamia New Delhi-110025
[2]P.G Student, Department of Mechanical Engineering Jamia Milia Islamia New Delhi-110025
E-mail: [1]rahim_ark@rediffmail.com , [2]sattudwi@gmail.com

Abstract—*A Computational attempt to investigate the drag and lift forces which are the critical factor for an aerodynamic body at different angle of attack (AOA) ranging from (-2° to 8°) and at Reynolds number of the order of $3x10^6$is made for a horizontal axis wind turbine blade. Airfoil NACA 65_3-218 with maximum thickness of 18% at 39.9% chord length is selected for the purpose and simulation is performed using Computational fluid Dynamics (CFD).The length of blade is taken as 37 meter which is standard designed blade of GE 1.5-77 1.5MW turbine. Pressure, Velocity and C_L/C_D contours for various, angle of attack are shown and are validated with experimental results as available in literatures and are found to be in sound similarity with the experimental results. CFD results offers the best measure to validate the results obtained from the complex, expensive and inclusive of state-of- the art infrastructure of wind tunnel testing experimental procedures. Also there are some analytical and semi-empirical models, feasibility of those models are insignificant and found to have less importance in the field of aerodynamic testing. A pressure difference in upper and lower surfaces of the airfoil is observed which generates the lift forces. Lift coefficient, drag coefficient and pitching moment are found to have increase with increase in angle of attack. An optimum angle of attack is observed at 5° where C_L/C_D value is maximum.*

1. Introduction

Horizontal axis wind turbines are one among the prominent devices in recent demands for sustainable development. "The increase in efficiency of existing turbines means that we could already generate nearly 50 percent more power just through higher towers and bigger rotors alone. Nevertheless there is still potential for optimization: for Onshore there is a realistic limit of 50 % and for offshore of 65 % in capacity factor" reported by Henrik Stiesdal [1] in recently concluded Global wind summit in Hamburg. Digitalization potential of wind energy is attracting more and more researchers for revolutionizing the renewable energy sector. Wind turbines has been subjected to expeditious growth in past decades and dependency of renewable energy sector in this area has been drastically increased. Numerical simulation of airfoil of wind turbine serve as a reference ground for further research and designing of airfoil. Blade design of any wind turbine is one

among crucial designing parameter because it is the part which is responsible for converting kinetic energy into mechanical energy. An optimum blade design for horizontal axis wind turbine is performed by Vitale et al.[2] using Blade element theory , a blade of NACA 2412 is chosen and rotor design procedures is implemented and rotor power and efficiency is validated with those provided by commercial manufactures and found to be similar. The aerodynamics performance of NACA 0018 is simulated numerically by Yao et al. [3] and lift and drag coefficient at different turbulence models is studied in detail with the help of CFD software. The attack angle is varied from -8° to 13°, a higher value of gradient of pressure coefficient at front edge of airfoil is observed whereas at large angle of attack the velocity gradient at front surface is higher. Sahin et al. [4] studied NACA 0015 at different attack angle (0° to 20°) and at low Reynolds number using CFD and concluded that lift and drag coefficient increases with increase in angle of attack and at 16° effect of stall is observed .A very recent study on Enhancement of Horizontal axis wind turbine performance by studying effect of winglet planform and winglet airfoil using Computational fluid dynamics is performed by Farhan et al. [5]. Nazmul haque et al. [6] experimentally shows that aerodynamic performance is enhanced by incorporating curved leading edge planform which is having higher lift to drag ratio. NACA 0013 is having optimum angle of attack at 21° and magnitude of lift force at that angle of angle of attack is 61,650 N reported by Hidayat et al. [7] using CFD ANSYS Fluent version 14.5 . k- Ω (SST) model is one of the frequently used models including 2 – transport equations as compared with other viscous models having generally 1-equation model,the transport variable k determines the energy and Ω determines the scale of turbulence .K- Ω is usually employed for boundary layer problems, where the formulation of inner part denotes the viscous layer ,it is the reason k- Ω (SST) model is used for low Reynolds flow applications without extra damping functions .k-ω (SST) is known for its excellent behavior in adverse pressure gradient and separating flows [8].SST model can

account for principal shear stress in adverse pressure gradient boundary layers [9]. Howell et al. [10] performed wind tunnel testing for Vertical axis wind turbine using 2D and 3D computational fluid dynamics models and it is established experimentally that surface roughness on turbine rotor blades has significant effect on performance and 2D simulations shows a significantly increased performance compared to 3D simulations. Srinivas et al. [11] studied drag, lift forces and the variation with angle of attack is shown, blade modelling is performed with the help of GAMBIT and solution is done in FLUENT at various angle of attack.

2. Governing Equations

2.1 Drag Forces (F_D)

It is defined as the parallel forces in the direction of oncoming airflow generated due to unequal pressure in upper and lower surfaces of airfoil , drag forces is attributed to both viscous friction forces at the surface of airfoil and pressure differential on the airfoil surfaces facing toward and away from the oncoming flow Manwell et al.[12].

$$F_D = \frac{1}{2}\rho A V^2 C_D, \quad C_D = \frac{F_D}{\frac{1}{2}\rho V^2} \quad (1)$$

2.2 Lift Forces (F_L)

It is defined as the perpendicular aerodynamic forces in the direction of oncoming air flow when angle of attack is not 0°, its tendency is to lift the body in upward direction. Lift occurs when a moving flow of gas is turned by a solid object. The flow is turned in one direction, and the lift is generated in the opposite direction.

$$F_L = \frac{1}{2}\rho A V^2 C_L, \quad C_L = \frac{F_L}{\frac{1}{2}\rho V^2} \quad (2)$$

2.3 Pitching Moment Coefficient (Cm)

It is defined as the moment produced by the aerodynamic force on an airfoil acting on an aerodynamic center Expression for pitching moment can be expressed as

$$C_m = \frac{M}{\frac{1}{2}\rho A V^2 C} \quad (3)$$

2.4 Mass Conservation Equation

Continuity equation or mass conservation can be written as

$$\frac{\partial \rho}{\partial t} + \nabla(\rho.\vec{v}) = S_m \quad (4)$$

Equation (4) is applicable for both compressible and incompressible flows. S_m is the mass added from continuous phase to dispersed second phase (e.g. due to vaporization of liquid droplets) and any user-defined sources.

2.5 Momentum Conservation Equation

Conservation of momentum in an inertial (non-accelerating) reference frame is described by

$$\frac{\partial}{\partial t}(\rho\vec{v}) + \vec{\nabla}(\rho.\vec{v}\vec{v}) = \vec{\nabla}p + \vec{\nabla}.\tau_{ij} + \rho\vec{g} + \vec{F}$$
(5)

In equation (5) p is the static pressure τ_{ij} is the stress tensors (described below) and $\rho\vec{g}$ is the gravitational body force and $\vec{F}$ is the external body force. Stress tensor is expressed as

$$\tau_{ij} = \mu[(\vec{\nabla v}+\vec{\nabla v}^T - \frac{2}{3}\nabla.\vec{v}I] \quad (6)$$

2.6 k-ω SST Model

Use of k-ω model in the inner parts of boundary layer makes the model very well suited for low-Reynolds turbulence model without need of any extra damping functions. The k-ω model is substantially more accurate than k-ε in the near wall layers, and has therefore been successful for flows with moderate adverse pressure gradients, but fails for flows with pressure induced separation [11].

2.6.1 Turbulence kinetic energy

$$\frac{\partial k}{\partial t} + U_J \frac{\partial k}{\partial x_j} = P_k \beta^* k\omega + \frac{\partial}{\partial x_j}[(\vartheta + \sigma_k\vartheta_t)\frac{\partial k}{\partial x_j}] \quad (7)$$

2.6.2 Specific dissipation rate

$$\frac{\partial \omega}{\partial t} + U_J \frac{\partial \omega}{\partial x_j} = \alpha s^2 \beta \omega^2 + \frac{\partial}{\partial x_j}[(\vartheta + \sigma_\omega\vartheta_t)\frac{\partial \omega}{\partial x_j}] + 2(1-F_1)\sigma_{\omega 2}\frac{1}{\omega}\frac{\partial k}{x_i}\frac{\partial \omega}{x_i} \quad (8)$$

Where F_1 = blending functions, F_1=1 inside the boundary & F_1=0 outside the boundary [13].

3. Problem Description

Geometry of designated airfoil is created in Design Modeler of ANSYS FLUENT 16.0.Co-ordinates of airfoil is imported from UIUC Airfoil Coordinate database in ANSYS modeler and then surface is created in X-Y plane around the co-ordinate points. 51 points are obtained for the airfoil NACA 65_3-218. Rotate function of design modeler is applied for tilting the airfoil to a desired angle of attack, for each angle of attack we have to change the rotate values normal to X-Y plane, other surfaces are created around the modeled airfoil in order to have best results in FLUENT in X-Y plane at different sketches and having predetermined dimensions. Edge split function is applied to differentiate edges of airfoil named as top and bottom for obtaining separate values for drag and lift at each portion , Boolean is applied to distinct the line body of airfoil from the other created surfaces for high resolution visualization in the CFD-post segment. At the end

of modeling we have one line body and three surface body. The modeling is transferred to meshing of ANSYS FLUENT 16.0. Meshing is performed with Relevance center as fine, Smoothing as high, Maximum face size and Max size as 0.10 meter etc. Body sizing is performed by selecting front surface as one body and other two created surfaces in body of influence with element size of 0.02 meter and Growth rate as 1.20 meter. Edges of airfoil named as top and bottom is selected in edge sizing and number of divisions as 250 and having hard behavior. Other left edges of airfoil is further selected in other edge sizing procedures and same parameters are implemented as performed before. Inflation is applied on the front face of the surface created around the airfoil for better results and total of four edges are selected with Maximum thickness 0.01 meter, Number of layers as 10 and growth rate is kept as 1.2 meters , Combination of octahedral and triangular meshes are visualized in the resulting mesh as shown in Fig 2. Mesh statistics shows that a skewness value of 0.9 to 0.99 is obtained for all meshes which is a parameter on a scale of 0 to 1, where value 1 represents for a high quality mesh.
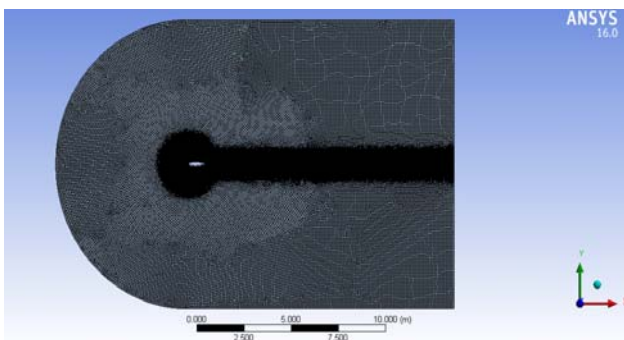

Figure 1: Meshing around NACA 65$_3$-218 airfoil

3.1 Boundary Conditions

For setup boundary conditions FLUENT Launcher on serial processor is employed, Pressure based and steady conditions are setup in Absolute velocity formulation. Viscous model of k-ω SST is utilized for better aerodynamic set of equations. Boundary conditions for no slip and turbulent intensity as 5 % and turbulent viscosity ratio as 10 is selected. Inlet velocity of the order of 10 m/s and a static pressure is chosen for the inlet and outlet boundaries with Mach number less than 0.1. A coupled scheme with a gradient of least square cell based, second order pressure and momentum as second order upwind to have better accuracy in solution methods. Drag & lift components of forces are added in Report definitions in X and Y directions and pitching moment is added in Z direction. Hybrid solution initialization is usually preferred for initialization purpose and suitable number of iterations is to be chosen for the optimal convergence of solution.

4. Results and Discussion

4.1 Contours of static pressure

Contours of static pressure from angle of attack -2° to 8° is shown in Fig. 2 to 4. It is evidently observed from the contours that pressure at the lower surface of the airfoil for the oncoming flow is more than the upper surface so that the incoming can effectively push the airfoil upward normal to the flow direction of air.
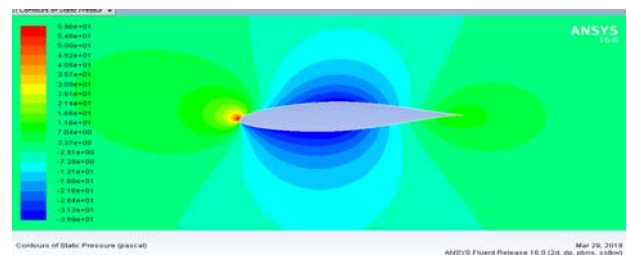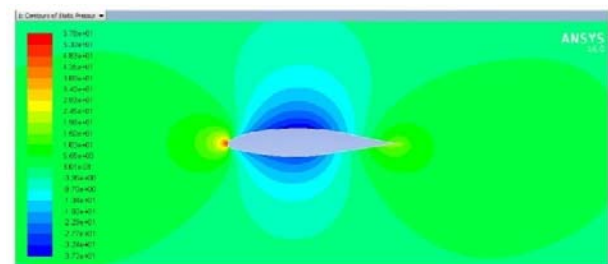

Figure 2: Static pressure contour at -2°

Figure 3: Static pressure contour at 0°

Suction pressure at the upper surface of airfoil which is lesser as compared with the lower surface of the airfoil as shown in Fig. 2 and 3, more and more air is pushes to down by the airfoil due to which a net upward force generation known as lift take place. As the air encounters the airfoil at the leading edge or nose the pressure is maximum at this point as shown in figure 3 and 4 the magnitude of pressure coefficient at this point is maximum. With increase of angle of attack from 4° to 6° the maximum pressure attained is slightly decreased showing the best or optimum angle of attack for the airfoil is 5°.
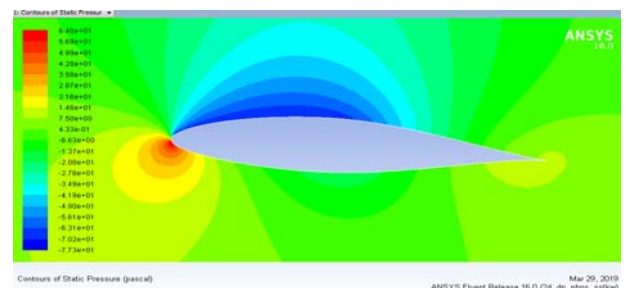

Figure 4: Static pressure contour at 4°

Phenomenon of pressure recovery is encountered during increase of pressure from its minimum value to the small positive value attained at the training edge of the airfoil.

4.2. Velocity contours

The contours of velocity is shown in Fig. 5 to 7. Velocity at upper surface of airfoil is greater than lower surfaces .Entering velocity is assumed in simulation as 10 m/sec and at upper surfaces the magnitude reach up to the order of nearly 19 m/sec. When the flow is just encountering the surface of the airfoil it has to part near the leading edge and pass along the upper and lower surface of the airfoil. At the point of separation where the flow is splitting up, at this accelerating type of flow the flow velocity is almost reduced to zero called as stagnation point as shown in Fig. 5 and 6.
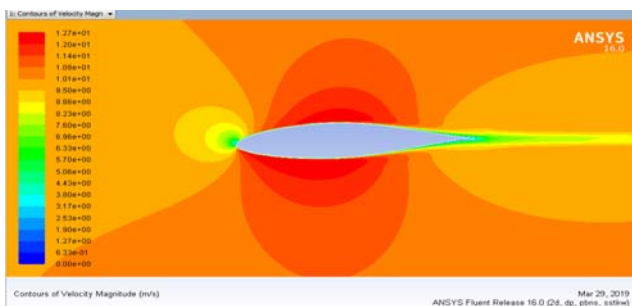
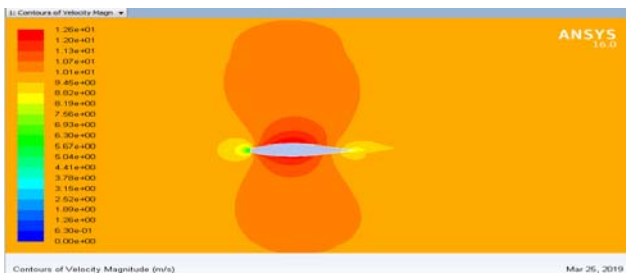

Figure 5: Velocity contour at -2°

Figure 6: Velocity contour at 0°

The position of stagnation point in Fig. 6 and 7 is not same this shows that this point moves with angle of attack.
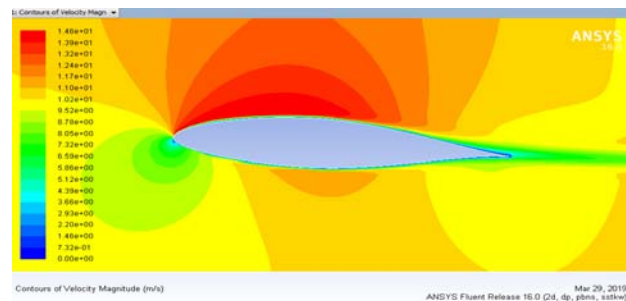

Fig 7: Velocity contour at 4°

Fig. 7 shows the flow field around an airfoil in which higher velocity at the upper surface of the airfoil as compared with the lower surface of airfoil is observed as evident from Bernoulli's equation that increasing the velocity decreases the local pressure and vice versa. Fig. 6 and 7 shows that on increasing the angle of attack velocity at upper surface increases, whereas the velocity on lower surface is slightly reduced which increases the lift coefficient.

4.3. Plots of pressure coefficient

X-Y plots for pressure distribution on top and lower surfaces of airfoil is depicted in Fig. 8 to 10.
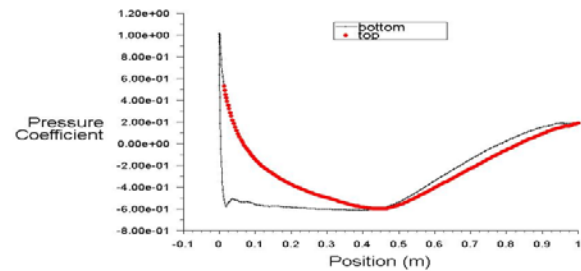

Figure 8: Pressure coefficient plot at -2°

Fig.8 shows the plot of pressure coefficient w.r.t position of the airfoil pressure at the leading and trailing edge is greater than the free stream whereas pressure in the upper and lower side is lower than free stream. Pressure coefficient at upper surfaces are found to have negative pressure coefficient showing the suction nature at these surfaces. Fig. 9 and 10 shows a substantial difference of pressure coefficient in top and bottom surfaces at leading edge of the airfoil showing that top surfaces have negative pressure coefficient which is due to higher air speed at these surfaces leading to conversion of free stream static pressure to kinetic energy of the air.
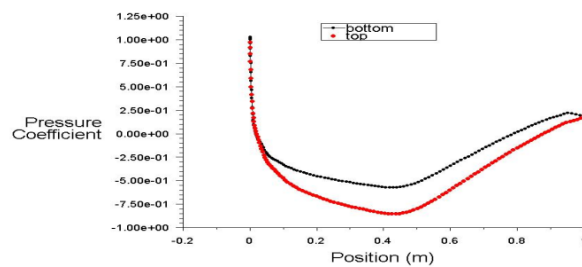

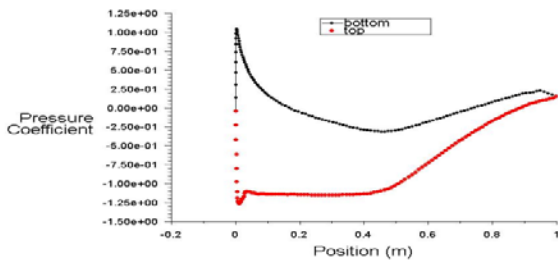**Figure 9: Pressure coefficient plot at 0°**

Figure 10: Pressure coefficient plot at 4°

In Fig. 9 and 10 sudden increase in value of pressure coefficient in suction side is observed this phenomenon is called as shock. For an airfoil designer the utmost important objective is to avoid boundary layer separation i.e. to keep the low pressure at upper surfaces. In case of deviation from this the pressure at lower surfaces decreases and effect of drag forces are more prominent leading to drastic losses in lift.
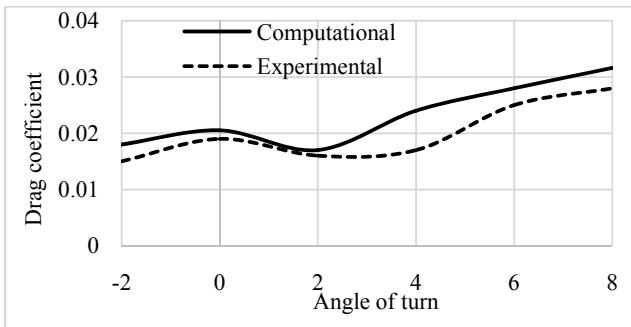

Figure 11: Curve of drag coefficient

Fig. 11 shows the linear increase of drag coefficient with angle of attack as the frontal surface area and boundary layer increases. An important thing to consider during designing of airfoil is to have avoid any stalling effect after which both lift and drag becomes unsteady. Fig. 12 shows the variation of lift coefficient with angle of attack, magnitude of lift generation for small angle of attack increases with increase in angle of attack. At higher angle of attack airfoil is more prone to stalling. More and more air is drawn downwards hence higher lift obtained during this region.
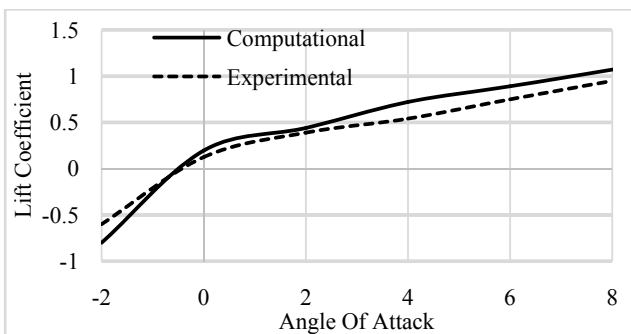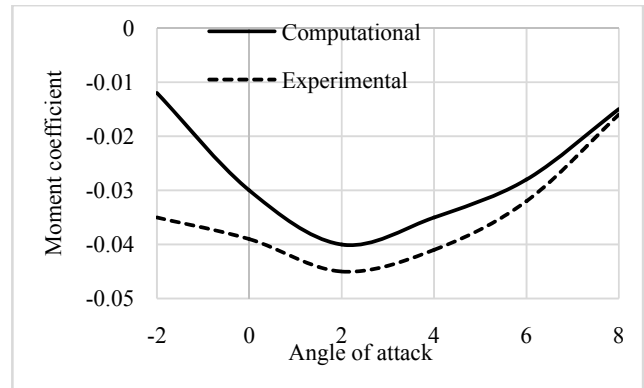

Figure 12: Curve of Lift coefficient

Figure 13: Curve of Pitching Moment coefficient

Pitching moment is the moment that acts on an airfoil at the aerodynamic center. Fig. 13 shows the pitching moment coefficient w.r.t angle of attack up to 2° with increase in angle of attack pitching moment coefficient decreases and after which an increasing trend is observed with increasing angle of attack. There Fig. 14 shows the C_L/C_D w.r.t angle of attack at 5° maximum ratio of C_L/C_D is obtained termed as optimum angle of attack.
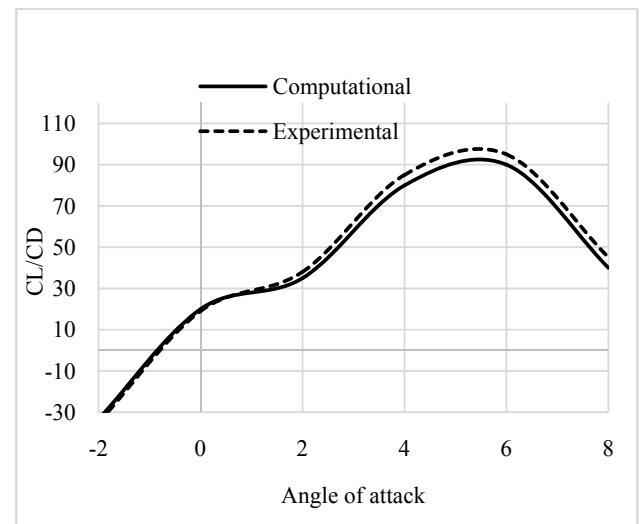

Figure 14: Curve of C_L/C_D

6. Conclusion

In the present work numerical simulation with the help of Computational Fluid dynamics is done in ANSYS Fluent 16.0. Validation of performed numerical simulation with experimental results is done as per Summary of Airfoil Data by Abbott et al. [14]. Viscous model for the present analysis is considered as k-ω SST model which is a two equation model. Result obtained from numerical simulation is then compared with experimental results available in literatures. Lift coefficient, drag coefficient is found to have increasing trend

with increase in angle of attack whereas pitching moment coefficient is first decreases up to angle of attack 3°and then increases with angle of attack. Best C_L/C_D value is obtained at 5° and considered to be most efficient angle of attack. Pressure at lower surfaces of airfoil is more than upper surfaces of airfoil and higher velocities is observed at upper surfaces of airfoil.

7. Nomenclature

HAWT- Horizontal Axis Wind Turbine

CFD - Computational Fluid Dynamics

NACA - National Advisory Committee for Aeronautics

C_L - Lift Coefficient

C_D - Drag Coefficient

C_m - Pitching Moment Coefficient

AOA - Angle Of Attack

C - Length of Chord (in m

α - Angle of Attack (in °)

V - Wind Velocity (m/sec)

F_D - Drag Coefficient

F_L - Lift Coefficient

A - Reference Area (in m^2)

ρ - Density (kg/m^3)

M - Pitching Moment (N/m)

References

[1] Henrik Stiesdal , Global wind energy summit (2018) September, Hamburg Germany**.**

[2] A.J .Vitale, A.P.Rossi ,"Computational method for the design of wind turbine blade",*International journal of energy*. 33(2008) .3466-3470.

[3] Ji Yaoa,Weibin Yuanb,jianliang Wanga ,Jianbin Xiec, Haipeng Zhoub,Mingjun Pengd,Yong Sun.," Numerical Simulation of aerodynamic performance for two Dimensional wind turbine airfoils", *International Conference on Advances in Computational Modeling and Simulation*. Procedia Engineering 31 (2012),80 – 86.

[4] Izzet Şahin &Adem Acir,"Numerical and Experimental Investigations of Lift and Drag Performances of NACA 0015 Wind Turbine Airfoil", *International Journal of Materials, Mechanics and Manufacturing*, Vol. 3, No. 1, February 2015, 22-25.

[5] A.FathanA.Hassanpour ,A.Burns, Y.Ghaffari Motlagh "Numerical study of effect of winglet planform and airfoil On a horizontal axis wind turbine performance", *Renewable energy*, volume 131, February (2019) 1255-1273.

[6] Nazmul Haque, Mohammad Ali, Ismat Ara ," Numerical study of effect of winglet planform and airfoil on a on a horizontal axis wind turbine performance", *Procedia Engineering*, 105 (2015) 232 – 240. Elsevier.

[7] M. Fajri Hidayat, Yos Nofendri ," Aerodynamic Study Airfoil NACA 0013 with Ansys Fluent",(2019).

[8] CFD online ,turbulence model ,mediawiki 2014 http://www.cfdonline.com/Wiki/Turbulence_freestreamboundaryconditions.

[9] Menter,Florian R,"Improved two-equation k-omega turbulence models for aerodynamic flows", (1992).

[10] Howell, R., Qin, N., Edwards, J., Durrani N"Wind tunnel and numerical study of a small vertical axis wind turbine,", *Renewable Energy*, 35 (2)(2010), 412- 422.

[11] Srinivas G , Mahesha G T, Chethan K N and Arjun N,, 2014, "Analysis of Wind Turbine *and Technolog*y E-ISSN 2277-4106, P-ISSN 347- 5161.

[12] F. Manwell, J.G. McGowan & A.L. Rogers, "Aerodynamics of Wind Turbine", *Wind Energy Explained-Theory Design and Application*, John Wiley & sons ltd (2002).

[13] ANSYS FLUENT 16.0, User's Guide, Fluent Inc., January (2015).

[14] Abbott I.H., Von Doenhoff A.E., Stivers L., NACA Report No. 824-Sumary of Airfoil Data, National Advisory Committee for Aeronautics.